Published in final edited form as:

Wiley Interdiscip Rev Nanomed Nanobiotechnol. 2015 November ; 7(6): 828–838. doi:10.1002/wnan.1337.

NIR Fluorescent Small Molecules for Intraoperative Imaging

Eric A. Owens,
Department of Chemistry, Georgia State University, Atlanta, Georgia 30303
eowens9@student.gsu.edu

Stephanie Lee,
Division of Hematology/Oncology, Department of Medicine, Beth Israel Deaconess Medical Center and Harvard Medical School, Boston, MA 02215, USA slee32@bidmc.harvard.edu

JungMun Choi,
Division of Hematology/Oncology, Department of Medicine, Beth Israel Deaconess Medical Center and Harvard Medical School, Boston, MA 02215, USA jchoi10@bidmc.harvard.edu

Maged Henary, and
Department of Chemistry, Georgia State University, Atlanta, Georgia 30303 mhenary1@gsu.edu

Hak Soo Choi
Division of Hematology/Oncology, Department of Medicine, Beth Israel Deaconess Medical Center and Harvard Medical School, Boston, MA 02215, USA Department of Cogno-Mechatronics Engineering, Pusan National University, Busan 609-735, South Korea
hchoi@bidmc.harvard.edu

Abstract

Recent advances in bioimaging and nanomedicine have permitted the exploitation of molecular optical imaging in image-guided surgery; however, the parameters mediating optimum performance of contrast agents are not yet precisely determined. To develop ideal contrast agents for image-guided surgery, we need to consider the following criteria: 1) excitation and emission wavelengths in the NIR window, 2) optimized optical characteristics for high *in vivo* performance, 3) overcoming or harnessing biodistribution and clearance, and 4) reducing nonspecific uptake. The design considerations should be focused on optimizing the optical and physicochemical property criteria. Biodistribution and clearance should first be considered because they mediate the

No conflict of interest.

Related Articles

DOI	Article title
10.1002/wnan.7	In vivo fluorescence imaging: a personal perspective
10.1002/wnan.77	Near infrared imaging with nanoparticles
10.1002/wnan.1212	Image guided resection of malignant gliomas using fluorescent nanoparticles.
10.1002/wnan.1188	Shedding light on nanomedicine
10.1002/wnan.139	Optical molecular imaging of atherosclerosis using nanoparticles: shedding new light on the darkness

fate of a contrast agent in the body such as how long after intravenous injection a contrast agent reaches the peak signal-to-background ratio (SBR) and how long the signal lasts (retention).

Keywords

Near-infrared fluorescence; Optical imaging; Signal-to-background ratio; Image-guided surgery

Introduction

Despite advancements in oral medications, surgery remains the primary treatment option for controlling the progression of many diseases from dysplasia to carcinoma.[1-3] Surgeons currently perform complex long-duration surgical resections without the aid of real-time image guidance. The common colloquialism we use for “extremely precise” is surgical precision, which is currently limited to anatomical structures and palpation with surgeons experience to perform complex surgeries.[4] There are times, especially in the resection of cancerous tissues, when eyesight alone is not enough to complete a complicated surgical resection successfully—we define successful as the complete removal of disease tissue and the avoidance of nerves, blood vessels, and other vital tissues.[5]

Surgeons currently utilize many pre-surgical imaging modalities including computed tomography (CT), magnetic Resonance Image (MRI), single-photon emission computed tomography (SPECT), or positron emission tomography (PET)[6-9] for deciphering the surgical field and for locating specific tissues, but subtle nuances after pre-surgical imaging can have severe consequences which could lead to additional surgical procedures, incomplete resection, poor patient outcomes or even death. It is undeniable that the development of biomedical imaging modalities has contributed significantly to the outcome of surgical procedures by locating the disease tissue prior to surgery. Unfortunately, the surgical field remains an ever-changing space where real-time imagery is required while the patient is undergoing an operation to minimize morbidity and mortality. To avoid this, we require the development of a real-time approach to the imaging of surgical field but there remain significant obstacles in developing successful optical contrast agents, including the high background associated with current molecular imaging technology.

High Background in Molecular Imaging

Molecular imaging exploits the radioactive property of various elements or compounds for visualization. Depending on the exact atomic or molecular characteristics, clinicians are able to observe the signal using positron or photon detecting equipment with appropriately radiolabeled contrast agents. In order for surgeons to clearly visualize their target, the molecular imaging contrast agent must offer high signal to background for optimum delineation of meaningful signal from surrounding tissue which offers a more precise image of the surgical field leading to increased surgical efficacy. Most clinically utilized contrast agents including ^{18}F-FDG (PET) or ^{99m}Tc (SPECT) to target diseased tissue with properly detectable signal, however, the percent injected dose (%ID) taken up by non-target (normal) tissue and organ remaining in the body after several hours of circulation and clearance is still high, i.e., nonspecific background. As shown in Figure 1,[5] elevated non-specific uptake of

the contrast agent makes deducing meaningful signal more difficult. The major organs including liver, kidneys, spleen and lung display equal or higher signals compared to the targeted tumor. Reducing the background associated with any contrast agent remains a paramount and very difficult research endeavor. The perfect contrast agent would exhibit high signal to background in the desired tissue with the remaining amount being cleared through renal filtration or hepatobiliary clearance with minimal off-target absorption.

Why Optical Imaging *via* Fluorescence?

Conventional PET scan, as shown in Figure 1, provides whole body imaging to find disease target, commonly using radiolabeled ^{18}F-FDG or other radioactive contrast agents such as ^{15}O, ^{11}C and ^{64}Cu.[10, 11] The proton-rich radionuclides spontaneously convert a proton to a neutron, resulting in the emission of a positron. This modality, similar to SPECT (usually exploits gamma rays emitted from ^{99m}Tc, ^{123}I, ^{111}In, ^{201}Tl, ^{67}Ga or ^{133}Xe) poses significant safety concerns and must be utilized sparsely to avoid unhealthy radiation exposure to the patient. MRI utilizes high magnetic fields to noninvasively image diseased and healthy tissues. Unfortunately, these various imaging techniques fail to offer the desirable spatial resolution required for operative guidance and translating the currently employed imaging technology into a real-time setting exposes the patient and surgical team to harmful levels of radiation during long-term procedures. Research endeavors are underway to develop a harmless and effective strategy for surgical imaging—one of the most promising methods is optical-based imaging using NIR fluorescence and herein we discuss the design concepts that must be considered for the development of these fluorescent compounds.

NIR Window of Optical Clarity

Molecular imaging encompasses a highly broad category of techniques that; however, a more specific type of molecular imaging, optical imaging, relies on the photophysical properties of a contrast agent to report, usually through fluorescence, on the location of the targeted tissue. Optical imaging allows for a very detailed image with high spatial resolution to be obtained in real-time if the correct imaging agents are utilized. Furthermore, optical imaging has been shown to be useful for image-guided surgery and allows target specific tissues inside the body using laser light excitation combined with corresponding fluorophores with excitation and emission in the NIR region of optical clarity. The NIR window is the optical range of the electromagnetic spectrum which is characterized by wavelengths between 650 nm and 900 nm and is depicted in Figure 2. Absorption and scattering properties of tissue greatly affects the photon penetration into living tissue; however, the NIR region of the electromagnetic spectrum overcomes this obstacle and can significantly improve *in vivo* imaging. Understanding the NIR window and the optimized excitation and emission wavelengths along with the molecular characteristics required for NIR wavelengths are key in developing ideal contrast agents for image-guided surgery.

There are several advantages of working in the NIR region of the spectrum. First, the endogenous chromophores present in living tissues absorb and scatter visible light, limiting light penetration to only a few millimeters. However, NIR light has a much lower tissue absorption coefficient, which permits its deeper penetration to several centimeters. Since common biological systems do not feature the capacity to absorb this wavelength of light it

is innocuous to human cells and tissue resulting in an inherently safer imaging modality. Additionally, the scattered light from the excitation source is greatly reduced in the NIR region since the scattering intensity is proportional to the inverse fourth power of the wavelength. Low background noise and low scattering of NIR fluorescence result in a high SBR, thereby allowing highly sensitive detection. Further advantages of NIR imaging includes low interferences from Raman scattering and reduced possibility of sample degradation.

Many biological compounds fluoresce within the ultraviolet (< 400 nm) and visible (400-650 nm) regions which makes observing contrast agents in this range nearly impossible; however, NIR-fluorescent compounds avoid this issue by being spectrally distinct from the native biological fluorescence (autofluorescence) which offers outstanding SBR. It has been convincingly demonstrated that native tissue greatly interferes with the extraction of meaningful signal in the red-shifted visible region. Therefore, the lower limit (> 650 nm) of the NIR window is bound by biological autofluorescence. The upper end of the NIR region (< 900 nm) of optical clarity is bound by absorption arising from vibrational characteristics of water (> 950 nm). These advantages along with the availability and low cost of long-wavelength diode lasers and detectors for the NIR light, have led to increasing research interest in the design, development, spectroscopic characterization and application of novel NIR fluorophores.[12]

Small Molecule Optical Contrast Agents

Engineering optical contrast agents that satisfy the physical, chemical and biological requirements is a difficult process but remains crucial in maximizing the surgical implementation of image-guided surgery.[13] The performance of contrast agents depends strongly on their physicochemical properties (i.e. molecular weight, total polar surface area, hydrogen bond donors/acceptors, acidic/basic pKa, distribution/partition coefficient and stability), which heavily influence their *in vivo* fate with slight structural modifications posing significant biological perturbation.[14-23]

Efficient optical properties are the very basic requirements for developing new contrast agents and there are several crucial parameters such as high solubility, high extinction coefficient, large Stokes' Shift, high quantum yield, and high photobleaching threshold that directly influence the potential obtainable signal during the imaging process.[24, 25] Correspondingly, the first essential task is to optimize these parameters in the process of developing novel contrast agents.

The aqueous optical profile and water solubility normally go hand-in-hand; therefore, the first design consideration is either to avoid a highly hydrophobic core or alternately incorporate a charged group onto the fluorophore. Following these design parameters drastically increases the aqueous solubility and can increase the quantum yield (up to 10x). Judicious placement of charge is necessary as superfluous intrinsic charge can reduce the efficacy of biological targeting moieties due to steric hindrance, electrostatic repulsion or general bio-incompatibility. Therefore, fluorophores should be designed to have high aqueous solubility, while maintaining target recognition.

Additionally large extinction coefficient and quantum yield values are paramount for optical contrast agents, especially at the tissue depths required for image-guided surgery. The extinction coefficient—measure of the absorption at a particular wavelength by a compound—accurately represents the ability of a compound to absorb radiation and can be determined using the Beer-Lambert equation[26]. For optical imaging, typical satisfactory extinction coefficients in aqueous systems are between 100,000 and 200,000 $M^{-1}cm^{-1}$. This range of extinction coefficients results in reasonable photon absorption by the fluorophore.

Last but not least, high photobleaching threshold is a very important area of consideration. Conventional fluorophores are highly susceptible to photobleaching which places severe limitation on the fluence rate and consequently the sensitivity and length of detection. For example, the NIR fluorescent indocyanine green (ICG) rapidly photobleaches in warm serum when fluence rates exceed 50 mW/cm^2 .[27] However, hybrid nanoparticles (quantum dots, etc.) and multivalent polymeric nanomaterials commonly have higher resistance to photobleaching compared to small molecules with ability to withstand fluence rates one to two orders of magnitude higher. Because yu fluence rates improve the signal-to-background, contrast agents with higher resistance to photobleaching will yield improved fluorophores.

Classes of NIR Fluorophores

Among the optical contrast agents explored to date, the NIR region has gained considerable numbers of ideal fluorophores with potential for translation in image-guided surgery. Fortunately, there are several classes of fluorophores that offer appealing characteristics for further modifications towards designing contrast agents within the NIR window. The general molecular structures seen in Figure 3 represent a selection of chromophores that fluoresce in the NIR region. These fluorophores have general properties that either make them more appealing or limit their overall utility as bioimaging agents.

Nile red and nile blue are notoriously solvatochromic (change absorption spectrum when changing solvent or environment), highly hydrophobic fluorophores that can be modified in several positions to achieve water solubility;[28] however, analogs synthesized and evaluated to date fluoresce in the NIR albeit with low quantum yield in aqueous systems or in the presence of proteins. These limitations have precluded them from being extensively evaluated *in vivo*.[29-32] Another class of compounds centers on the cyclic oxobutanal ring and is referred to as squaraine or squaric acid fluorophores.[33] The extreme electrophilicity of this cyclic butane ring is susceptible to nucleophilic attack, which irreversibly diminishes the optical properties of the compound, unless the core is protected by one of several methods including rotaxane encapsulation[34] which reduces the overall applicability in small molecule bioimaging. Contrary to the squaraine class of fluorophores, the tricyclic fused structures of phenoxazine and phenothiazine are highly structurally and optically stable even in the presence of nucleophilic species due to the aromatic core. The synthetic difficulty associated with this class limits the versatility and overall applicability in image-guided surgery. Furthermore, the emission wavelengths of the oxazine class is too low and cannot be used due to interfering native tissue absorption and autofluorescence.[35, 36] The boron-dipyrromethane (BODIPY) class of fluorophores exhibits excellent characteristics from high stability and above-average quantum yield but suffers from having a highly hydrophobic

core and broad absorption/emission spectra. These fluorophores have been successful *in vivo* due to their NIR emission, high quantum yield and ability to be synthetically tailored to several applications.[23, 37-41] currently, however, high background during intravenous injection limits the scope for this molecular class.[23]

Cyanine fluorophores are broadly defined as two heterocyclic nitrogen atoms that are connected *via* an electron deficient polymethine bridge. Monomethine cyanines display one methine unit, in this case defined as (=CH-), between the heterocyclic structures, this class of compounds displays absorbance within the ultraviolet and visible regions with low fluorescence quantum yield. Elongating the central chromophore length by sets of 2 methylene groups yields tri-, penta-, and heptamethine cyanines. The wavelengths of most trimethine cyanines are too low to be effective in NIR imaging in biological systems; however, penta- and heptamethine cyanines have near-infrared absorbance and fluorescence characteristics that are a function of their exact heterocyclic structure and moieties within the polymethine chain which can be tuned to offer high quantum yield and molecular brightness with a high degree of structural amenability toward manipulating the pharmacophore in the generation of successful NIR fluorescent contrast agents.

State-of-the-art in Image-Guided Surgery

Figure 4 shows two of the most highly used optical contrast agents, methylene blue (MB), a fused phenothiazine compound, and ICG, a heptamethine cyanine dye. Surgeons have found ways to utilize the FDA approved ICG;[42-47] however, the high background signal *in vivo*, structural and optical instability and the lack of ability for a targeting functionality has opened several avenues for the manipulation of the chemical structure. MB, perhaps the second most widely researched compound in image-guided surgery not because of its NIR fluorescence but its color staining properties[48, 49] unfortunately suffers from non-dependable optical properties.[50-57] The absorption and fluorescence characteristics are at appropriate wavelengths during *in vitro* experimentation; however, the redox state of the compound allows for the reduction of the central imine to the corresponding amine which destroys the NIR fluorescence of the compound. These non-optimum properties along with low extinction coefficient and non-amenability to the addition of a targeting ligand limit the overall utility of this particular contrast agent. In order to develop robust NIR fluorescent contrast agents for image guided surgery, the general structure of ICG was modified to include a central cyclic ring for increased optical and chemical stability along with a zwitterionic character to minimize cellular accumulation and prevent off-target localization. [14, 15] Additionally, a reactive carboxylate moiety was added for structural manipulation toward targeted imaging.[16] The engineered molecule is depicted in Figure 4 and is known as ZW800-1 and is among the carbocyanine class of NIR contrast agents for targeted imaging once conjugated to a biological targeting ligand.[16]

Background Retention

Optical contrast agents have been designed to satisfy the optical property criteria and their capacity to luminesce using fluorescence light through skin and tissue has been convincingly demonstrated, but only a few fluorophores exhibit the ultralow background required for clinical translation.[14-16, 25, 58-64] Obtaining this high signal to background depends on the

clearance pathway from the body and there are structural constraints that allow compounds to be cleared through renal filtration—the pathway for obtaining clear background.

Renal clearance, involving the kidney, is the ideal route as it minimizes retention and toxicity risks within the body.[65] There are three steps that comprise the process of renal clearance: glomerular filtration, tubular secretion, and urinary excretion.[66, 67] The molecular shape, conformation, size and surface charges are important determinants of renal clearance, more specifically glomerular filtration.[24] Intravascular agents with a hydrodynamic diameter (HD) smaller than 6 nm are usually successfully filtered when the surface charges are neutral or zwitterionic, while injected molecules with an HD > 8 nm are not filtered through kidneys at all.[58, 68] Large molecules or highly charged molecules undergo some level of hepatobiliary excretion, which generally involves catabolism and biliary excretion, and contaminates the gastrointestinal (GI) tract and increase non-specific uptake. Although the overall size is smaller than 6 nm, cationic charged molecules trap in the negatively charged filters and vasculature, and increase background signal significantly.

The comparison between ZW800-1 and ICG shows a prime example of the clearance pathway leading to elevated background signal. ZW800-1 displays unique and exciting biological and physiological properties *in vivo*.[14-16] The highly charged yet neutral character prevents cellular accumulation and minimizes protein interactions allowing for complete and rapid clearance through renal filtration as shown in comparison to ICG in Figure 5. The biodistribution pattern associated with ICG is more common among alternate NIR fluorophores with high non-specific uptake shown through the high signal in the liver and duodenum evidenced by the high fluorescence signal in Figure 5.

Nonspecific Uptake and Persistent Background Retention (PBR)

The focal point of optical imaging combined with appropriate contrast agents is to produce a high SBR: increase the target signal while decreasing the background signal and noise. While the focus of optical imaging is typically on generating signal, it is the SBR, and more often background, which dictates the performance of an injected contrast agent. From the moment an exogenous contrast agent is injected intravenously, it is likely non-specifically contributing to background signal and degrading overall performance. The SBR is adequate for imaging only after specific binding to the desired target and clearance of this non-specific background from tissue.

Although virtually all published mathematical models of contrast agent biodistribution and clearance suggest that background is cleared in a relatively short period of time, especially for small molecule contrast agents, in reality there is a phenomenon of persistent background retention (PBR) that results in 10-30% of the injected dose remaining non-specifically in tissues throughout the body.[69, 70]While the mechanism for PBR is presently unknown, it appears to be a strong function of molecular size, shape, charges, and charge-to-mass ratio.[24] Therefore, in order to improve the SBR of an injected molecule thus improve its intraoperative use, reducing PBR is desperately needed through structural manipulating of its size, charge, absorption and clearance as the rapid biodistribution and complete elimination.

Conclusions

Although surgery is the main path in curing almost half of all cancer patients, none can perfectly image the desired target due to high levels of background signal that results in extreme difficulty during surgery. Designing the best possible contrast agent is essential in maximizing the use of optical imaging to detect, target, and diagnose specific cancer cells *in vivo*. Therefore a thorough understanding of the molecular and tissue properties helps in designing the ideal contrast agent. Monitoring the surgical field though the visualization of near-infrared fluorescence stands firm as a leading alternative and arguably most viable option for real-time-guided surgery.

Acknowledgments

Further Reading/Resources

This study was supported by the NIH/NIBIB grant #R01-EB-011523 and the Dana Foundation Program in Brain and Immuno-Imaging; the contents of this paper are solely the responsibility of the authors and do not necessarily represent the official views of the NIH.

References

1. Fujimura M, Niizuma K, Endo H, Sato K, Inoue T, Shimizu H, Tominaga T. Quantitative analysis of early postoperative cerebral blood flow contributes to the prediction and diagnosis of cerebral hyperperfusion syndrome after revascularization surgery for moyamoya disease. Neurol Res. 2014 1743132814Y0000000432.
2. Nakahara M, Ito M, Hattori N, Magota K, Takahata M, Nagahama K, Sudo H, Kamishima T, Tamaki N, Iwasaki N. 18F-FDG-PET/CT better localizes active spinal infection than MRI for successful minimally invasive surgery. Acta Radiol. 2014
3. Mannu GS, Bhalerao A. A century of breast surgery: from radical to minimal. Can J Surg. 2014; 57:E147–148. [PubMed: 25078943]
4. Vahrmeijer AL, Hutteman M, van der Vorst JR, van de Velde CJ, Frangioni JV. Image-guided cancer surgery using near-infrared fluorescence. Nat Rev Clin Oncol. 2013; 10:507–518. [PubMed: 23881033]
5. Backer MV, Levashova Z, Patel V, Jehning BT, Claffey K, Blankenberg FG, Backer JM. Molecular imaging of VEGF receptors in angiogenic vasculature with single-chain VEGF-based probes. Nat Med. 2007; 13:504–509. [PubMed: 17351626]
6. Vag T, Slotta-Huspenina J, Rosenberg R, Bader FG, Nitsche U, Drecoll E, Rummeny EJ, Gaa J. Computerized analysis of enhancement kinetics for preoperative lymph node staging in rectal cancer using dynamic contrast-enhanced magnetic resonance imaging. Clin Imaging. 2014
7. Bal H, Guerin L, Casey ME, Conti M, Eriksson L, Michel C, Fanti S, Pettinato C, Adler S, Choyke P. Improving PET spatial resolution and detectability for prostate cancer imaging. Phys Med Biol. 2014; 59:4411–4426. [PubMed: 25049221]
8. Povoski SP, Hall NC, Martin EW Jr. Walker MJ. Multimodality approach of perioperative 18FFDG PET/CT imaging, intraoperative 18F-FDG handheld gamma probe detection, and intraoperative ultrasound for tumor localization and verification of resection of all sites of hypermetabolic activity in a case of occult recurrent metastatic melanoma. World J Surg Oncol. 2008; 6:1. [PubMed: 18186915]
9. Candell L, Campbell MJ, Shen WT, Gosnell JE, Clark OH, Duh QY. Ultrasound-guided methylene blue dye injection for parathyroid localization in the reoperative neck. World J Surg. 2014; 38:88–91. [PubMed: 24132819]
10. Lee S, Chen X. Dual-modality probes for in vivo molecular imaging. Molecular imaging. 2009; 8:87–100. [PubMed: 19397854]

11. Blasberg RG. In vivo molecular-genetic imaging: multi-modality nuclear and optical combinations. Nuclear medicine and biology. 2003; 30:879–888. [PubMed: 14698792]
12. Weissleder R. A clearer vision for in vivo imaging. Nature biotechnology. 2001; 19:316–317.
13. Lee JH, Park G, Hong GH, Choi J, Choi HS. Design considerations for targeted optical contrast agents. Quantitative imaging in medicine and surgery. 2012; 2:266–273. [PubMed: 23289086]
14. Choi HS, Nasr K, Alyabyev S, Feith D, Lee JH, Kim SH, Ashitate Y, Hyun H, Patonay G, Strekowski L, et al. Synthesis and in vivo fate of zwitterionic near-infrared fluorophores. Angewandte Chemie. 2011; 50:6258–6263. [PubMed: 21656624]
15. Hyun H, Bordo MW, Nasr K, Feith D, Lee JH, Kim SH, Ashitate Y, Moffitt LA, Rosenberg M, Henary M, et al. cGMP-Compatible preparative scale synthesis of near-infrared fluorophores. Contrast media & molecular imaging. 2012; 7:516–524. [PubMed: 22991318]
16. Choi HS, Gibbs SL, Lee JH, Kim SH, Ashitate Y, Liu F, Hyun H, Park G, Xie Y, Bae S, et al. Targeted zwitterionic near-infrared fluorophores for improved optical imaging. Nature biotechnology. 2013; 31:148–153.
17. Kim SH, Lee JH, Hyun H, Ashitate Y, Park G, Robichaud K, Lunsford E, Lee SJ, Khang G, Choi HS. Near-infrared fluorescence imaging for noninvasive trafficking of scaffold degradation. Scientific reports. 2013; 3:1198. [PubMed: 23386968]
18. Kim SH, Park G, Hyun H, Lee JH, Ashitate Y, Choi J, Hong GH, Owens EA, Henary M, Choi HS. Near-infrared lipophilic fluorophores for tracing tissue growth. Biomedical materials. 2013; 8:014110. [PubMed: 23353894]
19. Ashitate Y, Hyun H, Kim SH, Lee JH, Henary M, Frangioni JV, Choi HS. Simultaneous mapping of pan and sentinel lymph nodes for real-time image-guided surgery. Theranostics. 2014; 4:693–700. [PubMed: 24883119]
20. Choi HS. Nanoparticle assembly: building blocks for tumour delivery. Nature nanotechnology. 2014; 9:93–94.
21. Hyun H, Wada H, Bao K, Gravier J, Yadav Y, Laramie M, Henary M, Frangioni JV, Choi HS. Phosphonated Near-Infrared Fluorophores for Biomedical Imaging of Bone. Angewandte Chemie. 2014
22. Park MH, Hyun H, Ashitate Y, Wada H, Park G, Lee JH, Njiojob C, Henary M, Frangioni JV, Choi HS. Prototype nerve-specific near-infrared fluorophores. Theranostics. 2014; 4:823–833. [PubMed: 24955143]
23. Salim MM, Owens EA, Gao T, Lee JH, Hyun H, Choi HS, Henary M. Hydroxylated near-infrared BODIPY fluorophores as intracellular pH sensors. Analyst. 2014
24. Choi HS, Frangioni JV. Nanoparticles for biomedical imaging: fundamentals of clinical translation. Molecular imaging. 2010; 9:291–310. [PubMed: 21084027]
25. Choi HS, Liu W, Liu F, Nasr K, Misra P, Bawendi MG, Frangioni JV. Design considerations for tumour-targeted nanoparticles. Nature nanotechnology. 2010; 5:42–47.
26. Beckford G, Owens E, Henary M, Patonay G. The solvatochromic effects of side chain substitution on the binding interaction of novel tricarbocyanine dyes with human serum albumin. Talanta. 2012; 92:45–52. [PubMed: 22385806]
27. Yaqoob Z, McDowell E, Wu J, Heng X, Fingler J, Yang C. Molecular contrast optical coherence tomography: A pump-probe scheme using indocyanine green as a contrast agent. J Biomed Opt. 2006; 11:054017. [PubMed: 17092166]
28. Jose J, Ueno Y, Burgess K. Water-soluble Nile Blue derivatives: syntheses and photophysical properties. Chemistry. 2009; 15:418–423. [PubMed: 19025740]
29. Chen W, Sommerfeld M, Hu Q. Microwave-assisted nile red method for in vivo quantification of neutral lipids in microalgae. Bioresour Technol. 2011; 102:135–141. [PubMed: 20638272]
30. Kuramitz H, Piruska A, Halsall HB, Seliskar CJ, Heineman WR. Simultaneous multiselective spectroelectrochemical sensing of the interaction between protein and its ligand using the redox dye Nile blue as a label. Anal Chem. 2008; 80:9642–9648. [PubMed: 19072269]
31. Sharma AK, Ahlawat DS, Mohan D, Singh RD. Concentration-dependent energy transfer studies in ternary dye mixture of Stilbene-420, Coumarin-540 and Nile Blue. Spectrochim Acta A Mol Biomol Spectrosc. 2009; 71:1631–1633. [PubMed: 18930436]

32. Lin CW, Shulok JR, Wong YK, Schanbacher CF, Cincotta L, Foley JW. Photosensitization, uptake, and retention of phenoxazine Nile blue derivatives in human bladder carcinoma cells. Cancer Res. 1991; 51:1109–1116. [PubMed: 1847656]
33. Sreejith S, Divya KP, Ajayaghosh A. A near-infrared squaraine dye as a latent ratiometric fluorophore for the detection of aminothiol content in blood plasma. Angew Chem Int Ed Engl. 2008; 47:7883–7887. [PubMed: 18781571]
34. Hsueh SY, Lai CC, Liu YH, Wang Y, Peng SM, Chiu SH. Protecting a squaraine near-IR dye through its incorporation in a slippage-derived [2]rotaxane. Org Lett. 2007; 9:4523–4526. [PubMed: 17914834]
35. Nowakowska-Oleksy A, Soloducho J, Cabaj J. Phenoxazine based units--synthesis, photophysics and electrochemistry. J Fluoresc. 2011; 21:169–178. [PubMed: 20625802]
36. Karlsson KM, Jiang X, Eriksson SK, Gabrielsson E, Rensmo H, Hagfeldt A, Sun L. Phenoxazine dyes for dye-sensitized solar cells: relationship between molecular structure and electron lifetime. Chemistry. 2011; 17:6415–6424. [PubMed: 21509836]
37. Carlson JC, Meimetis LG, Hilderbrand SA, Weissleder R. BODIPY-tetrazine derivatives as superbright bioorthogonal turn-on probes. Angew Chem Int Ed Engl. 2013; 52:6917–6920. [PubMed: 23712730]
38. Ucuncu M, Emrullahoglu M. A BODIPY-based reactive probe for the detection of Au(III) species and its application to cell imaging. Chem Commun (Camb). 2014; 50:5884–5886. [PubMed: 24760320]
39. Quan L, Sun T, Lin W, Guan X, Zheng M, Xie Z, Jing X. BODIPY fluorescent chemosensor for Cu2+ detection and its applications in living cells: fast response and high sensitivity. J Fluoresc. 2014; 24:841–846. [PubMed: 24522344]
40. Misra R, Jadhav T, Dhokale B, Gautam P, Sharma R, Maragani R, Mobin SM. Carbazole-BODIPY conjugates: design, synthesis, structure and properties. Dalton Trans. 2014; 43:13076–13086. [PubMed: 25043199]
41. Zhang HX, Chen JB, Guo XF, Wang H, Zhang HS. Highly sensitive determination of nitric oxide in biologic samples by a near-infrared BODIPY-based fluorescent probe coupled with high-performance liquid chromatography. Talanta. 2013; 116:335–342. [PubMed: 24148412]
42. Gilmore DM, Khullar OV, Gioux S, Stockdale A, Frangioni JV, Colson YL, Russell SE. Effective low-dose escalation of indocyanine green for near-infrared fluorescent sentinel lymph node mapping in melanoma. Ann Surg Oncol. 2013; 20:2357–2363. [PubMed: 23440551]
43. Hutteman M, Mieog JS, van der Vorst JR, Liefers GJ, Putter H, Lowik CW, Frangioni JV, van de Velde CJ, Vahrmeijer AL. Randomized, double-blind comparison of indocyanine green with or without albumin premixing for near-infrared fluorescence imaging of sentinel lymph nodes in breast cancer patients. Breast Cancer Res Treat. 2011; 127:163–170. [PubMed: 21360075]
44. Schaafsma BE, Mieog JS, Hutteman M, van der Vorst JR, Kuppen PJ, Lowik CW, Frangioni JV, van de Velde CJ, Vahrmeijer AL. The clinical use of indocyanine green as a near-infrared fluorescent contrast agent for image-guided oncologic surgery. J Surg Oncol. 2011; 104:323–332. [PubMed: 21495033]
45. Tummers QR, Verbeek FP, Prevoo HA, Braat AE, Baeten CI, Frangioni JV, van de Velde CJ, Vahrmeijer AL. First Experience on Laparoscopic Near-Infrared Fluorescence Imaging of Hepatic Uveal Melanoma Metastases Using Indocyanine Green. Surg Innov. 2014
46. van der Vorst JR, Hutteman M, Mieog JS, de Rooij KE, Kaijzel EL, Lowik CW, Putter H, Kuppen PJ, Frangioni JV, van de Velde CJ, et al. Near-infrared fluorescence imaging of liver metastases in rats using indocyanine green. J Surg Res. 2012; 174:266–271. [PubMed: 21396660]
47. van der Vorst JR, Schaafsma BE, Verbeek FP, Hutteman M, Mieog JS, Lowik CW, Liefers GJ, Frangioni JV, van de Velde CJ, Vahrmeijer AL. Randomized comparison of near-infrared fluorescence imaging using indocyanine green and 99(m) technetium with or without patent blue for the sentinel lymph node procedure in breast cancer patients. Ann Surg Oncol. 2012; 19:4104–4111. [PubMed: 22752379]
48. Gioux S, Choi HS, Frangioni JV. Image-guided surgery using invisible near-infrared light: fundamentals of clinical translation. Molecular imaging. 2010; 9:237–255. [PubMed: 20868625]

49. Merian J, Gravier J, Navarro F, Texier I. Fluorescent nanoprobes dedicated to in vivo imaging: from preclinical validations to clinical translation. Molecules. 2012; 17:5564–5591. [PubMed: 22576228]
50. Guay J, Grabs D. A cadaver study to determine the minimum volume of methylene blue or black naphthol required to completely color the nerves relevant for anesthesia during breast surgery. Clin Anat. 2011; 24:202–208. [PubMed: 21322042]
51. Moll X, Garcia F, Ferrer RI, Santos L, Aguilar A, Andaluz A. Distribution of methylene blue after injection into the epidural space of anaesthetized pregnant and non-pregnant sheep. PLoS One. 2014; 9:e92860. [PubMed: 24709655]
52. Shah-Khan MG, Lovely J, Degnim AC. Safety of methylene blue dye for lymphatic mapping in patients taking selective serotonin reuptake inhibitors. Am J Surg. 2012; 204:798–799. [PubMed: 22575397]
53. Ashitate Y, Lee BT, Laurence RG, Lunsford E, Hutteman M, Oketokoun R, Choi HS, Frangioni JV. Intraoperative prediction of postoperative flap outcome using the near-infrared fluorophore methylene blue. Ann Plast Surg. 2013; 70:360–365. [PubMed: 22395044]
54. Matsui A, Tanaka E, Choi HS, Kianzad V, Gioux S, Lomnes SJ, Frangioni JV. Real-time, near-infrared, fluorescence-guided identification of the ureters using methylene blue. Surgery. 2010; 148:78–86. [PubMed: 20117811]
55. Tummers QR, Verbeek FP, Schaafsma BE, Boonstra MC, van der Vorst JR, Liefers GJ, van de Velde CJ, Frangioni JV, Vahrmeijer AL. Real-time intraoperative detection of breast cancer using near-infrared fluorescence imaging and Methylene Blue. Eur J Surg Oncol. 2014; 40:850–858. [PubMed: 24862545]
56. van der Vorst JR, Schaafsma BE, Verbeek FP, Swijnenburg RJ, Tummers QR, Hutteman M, Hamming JF, Kievit J, Frangioni JV, van de Velde CJ, et al. Intraoperative near-infrared fluorescence imaging of parathyroid adenomas with use of low-dose methylene blue. Head Neck. 2014; 36:853–858. [PubMed: 23720199]
57. Verbeek FP, van der Vorst JR, Schaafsma BE, Swijnenburg RJ, Gaarenstroom KN, Elzevier HW, van de Velde CJ, Frangioni JV, Vahrmeijer AL. Intraoperative near infrared fluorescence guided identification of the ureters using low dose methylene blue: a first in human experience. J Urol. 2013; 190:574–579. [PubMed: 23466242]
58. Choi HS, Liu W, Misra P, Tanaka E, Zimmer JP, Itty Ipe B, Bawendi MG, Frangioni JV. Renal clearance of quantum dots. Nature biotechnology. 2007; 25:1165–1170.
59. Ashitate Y, Stockdale A, Choi HS, Laurence RG, Frangioni JV. Real-time simultaneous near-infrared fluorescence imaging of bile duct and arterial anatomy. The Journal of surgical research. 2012; 176:7–13. [PubMed: 21816414]
60. Wu Z, Shao P, Zhang S, Bai M. Targeted zwitterionic near infrared fluorescent probe for improved imaging of type 2 cannabinoid receptors. Journal of biomedical optics. 2014; 19:36006. [PubMed: 24604536]
61. Liu J, Yu M, Ning X, Zhou C, Yang S, Zheng J. PEGylation and zwitterionization: pros and cons in the renal clearance and tumor targeting of near-IR-emitting gold nanoparticles. Angewandte Chemie. 2013; 52:12572–12576. [PubMed: 24123783]
62. Liu J, Yu M, Zhou C, Yang S, Ning X, Zheng J. Passive tumor targeting of renal-clearable luminescent gold nanoparticles: long tumor retention and fast normal tissue clearance. Journal of the American Chemical Society. 2013; 135:4978–4981. [PubMed: 23506476]
63. Zhou C, Long M, Qin Y, Sun X, Zheng J. Luminescent gold nanoparticles with efficient renal clearance. Angewandte Chemie. 2011; 50:3168–3172. [PubMed: 21374769]
64. van Dam GM, Themelis G, Crane LM, Harlaar NJ, Pleijhuis RG, Kelder W, Sarantopoulos A, de Jong JS, Arts HJ, van der Zee AG, et al. Intraoperative tumor-specific fluorescence imaging in ovarian cancer by folate receptor-alpha targeting: first in-human results. Nature medicine. 2011; 17:1315–1319.
65. Longmire M, Choyke PL, Kobayashi H. Clearance properties of nano-sized particles and molecules as imaging agents: considerations and caveats. Nanomedicine. 2008; 3:703–717. [PubMed: 18817471]

66. Deen WM, Lazzara MJ, Myers BD. Structural determinants of glomerular permeability. Am J Physiol Renal Physiol. 2001; 281:F579–596. [PubMed: 11553505]

67. Ohlson M, Sorensson J, Haraldsson B. A gel-membrane model of glomerular charge and size selectivity in series. Am J Physiol Renal Physiol. 2001; 280:F396–405. [PubMed: 11181401]

68. Moghimi SM, Hunter AC, Murray JC. Long-circulating and target-specific nanoparticles: theory to practice. Pharmacological reviews. 2001; 53:283–318. [PubMed: 11356986]

69. Le Mignon MM, Chambon C, Warrington S, Davies R, Bonnemain B. Gd-DOTA. Pharmacokinetics and tolerability after intravenous injection into healthy volunteers. Investigative radiology. 1990; 25:933–937. [PubMed: 2394577]

70. van Hagen PM, Breeman WA, Bernard HF, Schaar M, Mooij CM, Srinivasan A, Schmidt MA, Krenning EP, de Jong M. Evaluation of a radiolabelled cyclic DTPA-RGD analogue for tumour imaging and radionuclide therapy. International journal of cancer. Journal international du cancer. 2000; 90:186–198. [PubMed: 10993959]

Sidebar title: Signal-to-Background Ratio (SBR) or Signal-to-Noise Ratio (SNR)

[SBR or SNR is of significant importance in molecular imaging, and many efforts have been focused to improve SBR for better targeting and imaging. The use of NIR fluorescence light is an important approach to lower background signal (autofluorescence) because absorption and scatter are low in the NIR wavelength range, photon attenuation is minimized and target detection up to 5 mm below the tissue surface is possible. Because autofluorescence is low in the NIR window, so too is the background on which targets are detected. Also the use of a right NIR fluorophore improves SBR to the target by lowering non-specific binding in the reticuloendothelial system (mononuclear phagocyte system; macrophage system) with efficient biodistribution and clearance.]

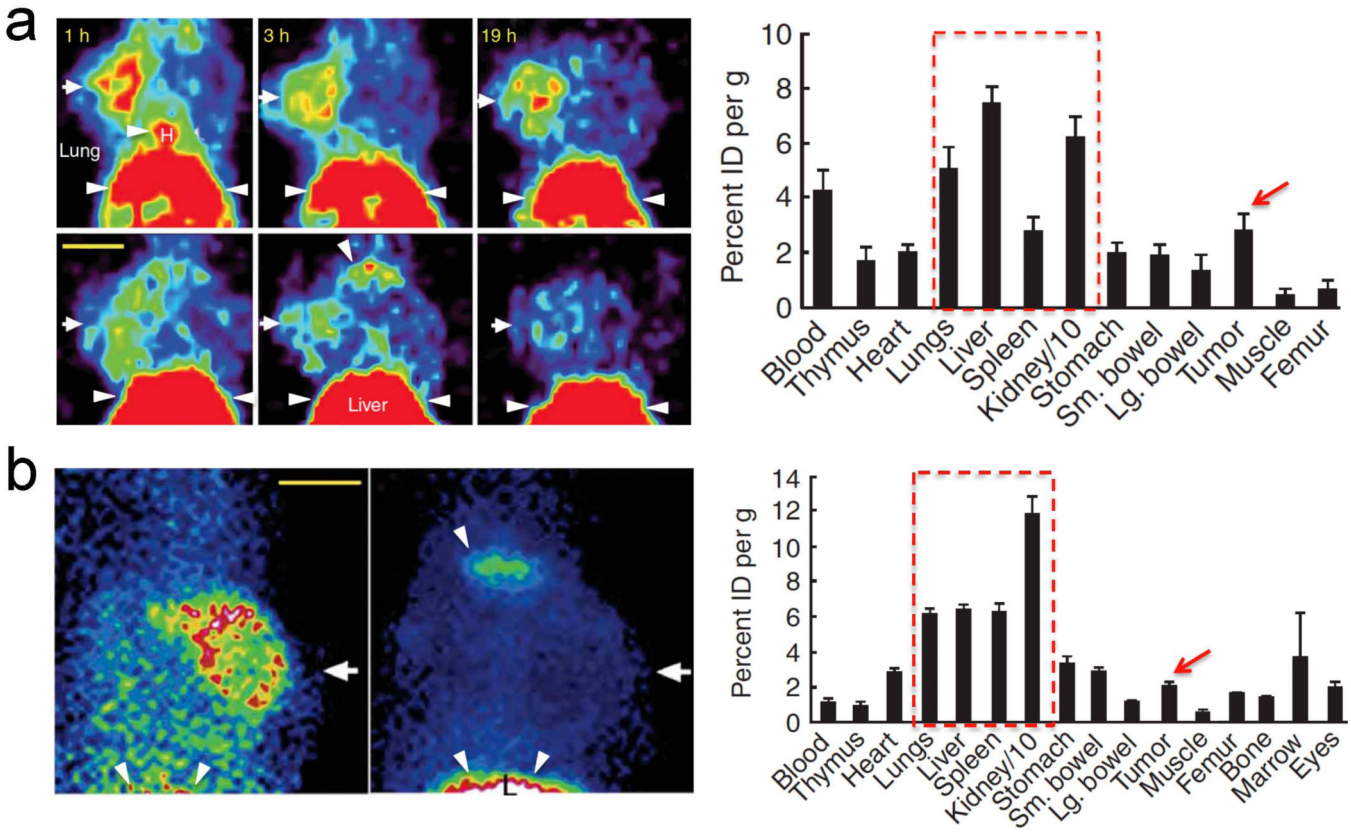

Figure 1.

(a) PET imaging. 100 μCi of scVEGF/Cu (top row) or inVEGF/Cu (bottom row) were injected into 4T1luc tumor-bearing mice in the left axillary fat pads. Radioactivity for each resected organ was obtained 2 h post-injection. (b) SPECT imaging. 100 μCi of scVEGF/Tc (left) or inVEGF/Tc (right) were injected into 4T1luc tumor-bearing mice 1 h prior to imaging and resection. Arrows mark left mammary fat pad tumor; arrowheads and dotted boxes indicate nonspecific uptake. H, heart; L, liver; scale bar, 1 cm [Adapted from Backer *et al.*[5] Copyright permission from Nature Publishing Group].

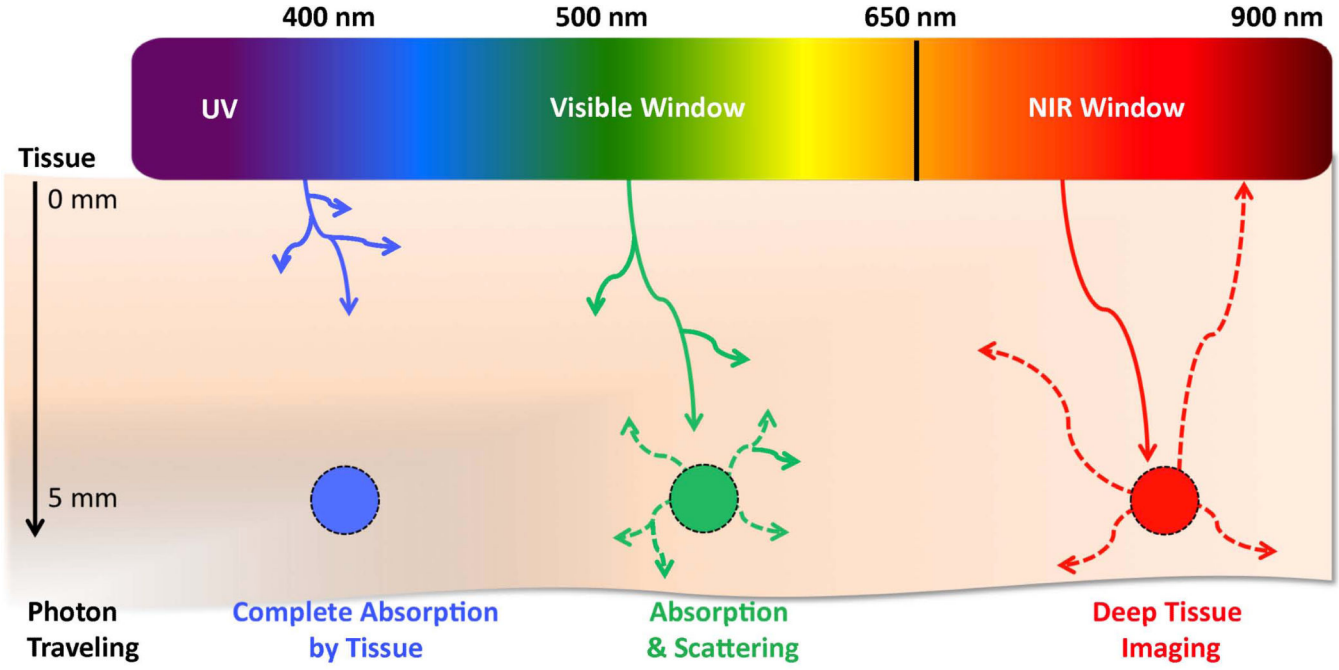

Wavelength (nm)	< 400	400 – 650	650 – 900
Spectrum	Ultraviolet	Visible	Near-infrared
Excitation Laser	None	Low	High
Absorption & Scatter	Very High	High	Low
Photon Emission	None	Low	High
Autofluorescence	High	High	Low
Cyanine Fluorophores	None	Mono-/Trimethine	Penta-/Heptamethine

Figure 2.
In vivo optical properties of injected fluorophores along with wavelength.

Fluorophore	Chemical Structure	Hydrophobicity	General Characteristics	Wavelength, Φ, ε
Nile Red (X = O) Nile Blue (X = NH_2^+)	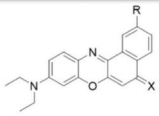	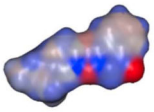	Highly solvatochromic and hydrophobic. Φ varies greatly according to R. Biodistribution is mostly unknown. Low modification potential.	X = O 530-600 nm, 40-80%, 60,000 $M^{-1}cm^{-1}$ X = NH_2^+ 530-600 nm, 40-80%, 60,000 $M^{-1}cm^{-1}$
Squaric Acid Fluorophores	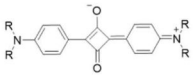	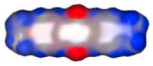	High Φ and ε (molecular brightness). High yielding synthetic routes with large opportunity of modification. Not stable in the presence of proteins.	600-650 nm, 50-80%, 250,000 $M^{-1}cm^{-1}$
Phenoxazine (X = O) Phenothiazine (X = S)	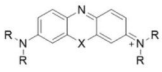	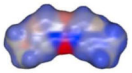	Structurally stable molecules that are generally synthetically low yielding. Low modification potential.	X = O 550-600 nm, 25-35%, 80,000 $M^{-1}cm^{-1}$ X = S 640-680 nm, 9-15%, 45,000 $M^{-1}cm^{-1}$
Boron-dipyrromethene (BODIPY)			Structurally stable but exhibits a broad abs spectrum with low Φ and ε. Highly amenable to diverse modifications.	480-750 nm, 15-35%, 80,000 $M^{-1}cm^{-1}$
Pentamethine Cyanine Dyes	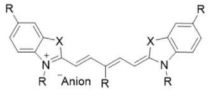	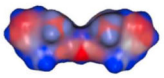	Structurally stable with comparatively high molar absorptivity and moderate quantum yield dependent on Rs. Highly modifiable.	650-700 nm, 20-60%, 200,000 $M^{-1}cm^{-1}$
Heptamethine Cyanine Dyes	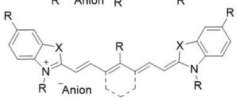	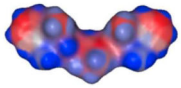	Structurally stable with central cyclic ring but otherwise chemically labile. Optical properties depend on Rs. Highly modifiable.	740- 850 nm, 12-40%, 200,000 $M^{-1}cm^{-1}$

Φ = quantum yield; ε = extinction coefficient

Figure 3.

Chemical structures of various classes of small molecule fluorophores that have been explored for biophotonic imaging, their general hydrophobicity maps, highlighted characteristics concerning their potential for in vivo performance and the overall optical properties concerning the general core structure.

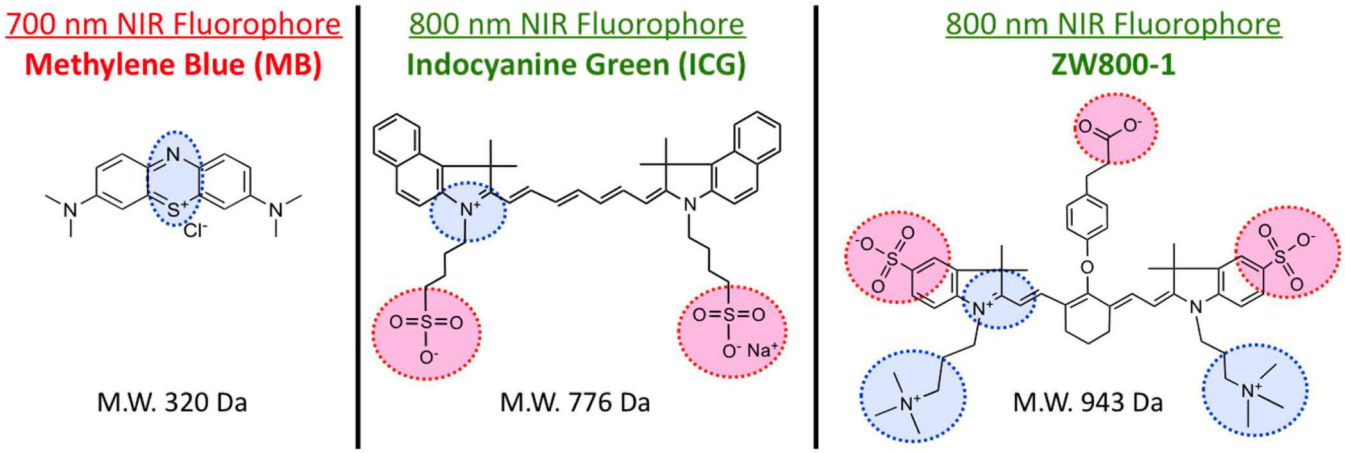

Optical Property	MB	ICG	ZW800-1
Peak λ_{ex} (nm)	665	807	772
Peak λ_{em} (nm)	688	822	788
Extinction Coefficient (ε, $M^{-1}cm^{-1}$)	49,500	121,000	249,000
Quantum Yield (ϕ, %)	9.6	9.3	15.1
Quenching Threshold (μM)	20	10	10
Molecular Brightness ($\varepsilon \times \phi$, $M^{-1}cm^{-1}$)	4,752	11,253	37,599

Figure 4.

Current state-of-the-art NIR fluorophores used in image-guided surgery. The chemical structures of three NIR fluorescent contrast agents and the corresponding optical properties. The negatively charged moieties are highlighted in red and the positively charged regions are designated in blue.

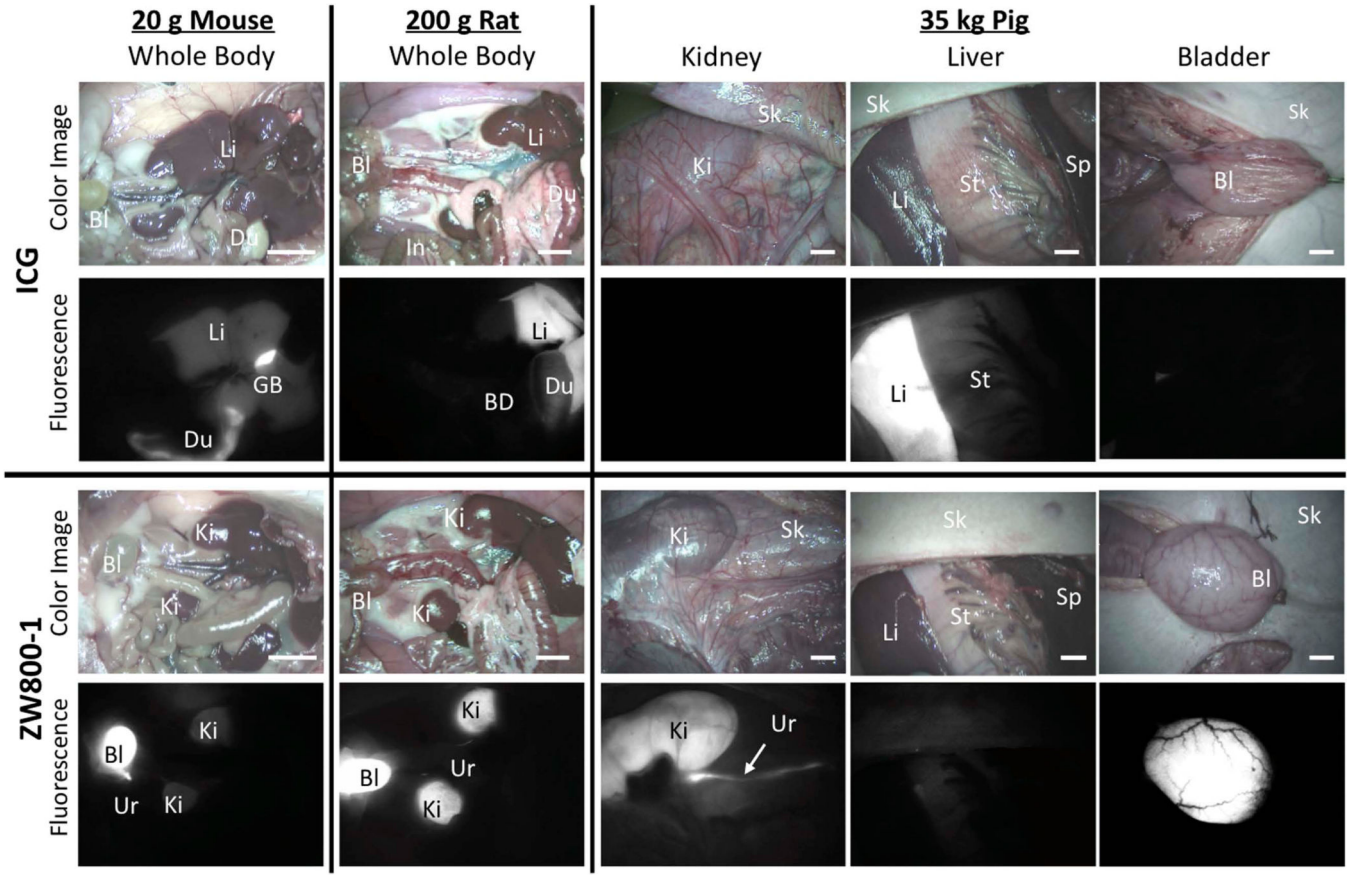

Figure 5.

Biodistribution and clearance of ICG and ZW800-1. ICG shows elevated nonspecific uptake in liver and duodenum, while ZW800-1 represents ultralow background and renal clearance. Animals were housed in an AAALAC-certified facility and were studied under the supervision of BIDMC IACUC in accordance with approved institutional protocols (#101-2011 for rodents and #046-2010 for pigs). NIR fluorophores were injected intravenously into ~20 g CD-1 mice (10 nmol), ~250 g SD rats (50 nmol), and ~35 kg Yorkshire pigs (1 μmol) 1 h prior to imaging. Shown are color and 800 nm NIR fluorescence images of surgically exposed organs taken by the FLARE intraoperative imaging system.[14-16] NIR fluorescence images have identical exposure times and normalizations. Abbreviations used are: Bl: bladder; BD: bile duct; Du: duodenum; In: intestine; Ki: kidneys; Li: liver; Sk: skin; St: stomach; Ur: ureter. Scale bars = 1 cm.